Scientia Iranica A (2013) 20(5), 1415–1432

Sharif University of Technology
**Scientia Iranica**
*Transactions A: Civil Engineering*
www.scientiairanica.com

# An enhanced particle swarm optimization for design of pin connected structures

**A. Baghlani*** **and M.H. Makiabadi**

*Faculty of Civil and Environmental Engineering, Shiraz University of Technology, Shiraz, Iran.*

Received 14 October 2012; received in revised form 14 January 2013; accepted 23 February 2013

**KEYWORDS**
Pin-connected structures;
Trusses;
Structural analysis;
Weight optimization;
Particle Swarm Optimization (PSO).

**Abstract.** In this paper, a new technique in weight optimization of pin-connected structures is proposed. Using some principles of structural analysis, the concepts of similar trusses in structural analysis and optimum similar trusses in optimization of truss structures are introduced. Based on these definitions, the technique searches for one of the optimum similar trusses to map it into boundary and find the optimum truss. The technique is referred to as Searching Optimum Similar Trusses (SOST). It is general and its implementation in standard Particle Swarm Optimization (PSO) is developed in this article, which is called PSOST. Rapid convergence with few numbers of analyses and accurate constraint handling is achieved by the technique, and absolutely feasible solutions are obtained. Several benchmark planar and spatial truss structures have been optimized using this approach. The results show remarkable improvement both in accuracy and particularly in convergence rate of the design.



## 1. Introduction

Structural optimization has been a very attractive and fast developing subject for decades. Pin-connected structures such as trusses or space frames are among the most widely used structures, and many efforts can be found in the literature concerning their optimization, using various optimization methods such as Genetic Algorithm (GA) [1-11], Ant Colony Optimization (ACO), [12-15] Harmony Search technique (HS) [16-20], simulated annealing [21,22] and other approaches [23-28]. In addition to aforementioned methods, Particle Swarm Optimization (PSO), which was first proposed by Kennedy and Eberhart [29], is one of the most powerful and competitive approaches. PSO has some remarkable advantages in comparison with other optimization algorithms; it is robust and efficient with suitable convergence rate [30]. It can also handle both continuous and discrete variables [30,31]. Compared to evolutionary algorithms such as GA, particle swarm optimization is much easier to implement in computer codes, since no binary encoding, crossover and mutation are required in the procedure [32]. Accordingly, many researchers have adopted PSO for optimization of truss structures [33-39].

Owing to the fact that the cost of a structure is proportional to its weight, most optimization approaches rely on minimizing the weight of structure as the objective function. Hence, for a given topology and configuration, the cross sections of the structure members are usually considered as optimization variables [7,16,20,26,28,35,37,39]. In other researches, topology and shape optimization of pin-connected structures have been studied [2,3,9,33]. Regardless of the type of the objective function considered in truss optimization, some constraints such as maximum displacement or stress constraints should be satisfied. Constraint

*. *Corresponding author. Tel: 0098 917 7101923; Fax: 0098 711 7264102*
*E-mail addresses: baghlani@sutech.ac.ir (A. Bghlani), h.makiabadi@sutech.ac.ir (M.H. Makiabadi)*

handling in such constrained optimization problems is a challenging topic. Despite its simplicity, standard penalty function approach often generates solutions which are infeasible to some extent. Most of the time, other techniques, such as fly-back mechanism proposed by He et al. [35], undergo a similar problem. On the other hand, most metaheuristic optimization methods are computationally expensive and practically ineffective for large and complex structures. Hence, expediting their rate of convergence is crucial to solve practical problems.

Recently, some researchers have attempted to modify the standard particle swarm optimization method to improve the convergence rate and accuracy of the algorithm in optimizing truss structures. He et al. [40] tried to improve the standard PSO, using Passive Congregation (PSOPC), and concluded that their approach was capable of enhancing both accuracy and rate of convergence of standard PSO. Kaveh and Talataheri [41] combined the PSOPC with ACO and Harmony Search scheme (HS) to reach an efficient method in weight optimization of truss structures, which was named HPSACO. Li et al. [37] proposed a Heuristic Particle Swarm Optimization (HPSO) with making use of PSOPC and harmony search scheme. They improved the convergence rate of standard PSO and PSOPC by their proposed approach.

In this study, an efficient and fast converging strategy is proposed to improve accuracy of the solution in satisfying design constraints and rate of convergence of iterative optimization algorithms in weight optimization of pin-connected structures. Using some principles of structural analysis, the concept of similar trusses is first introduced in this context. Optimum similar trusses are then defined in the context of truss optimization. The effectiveness of these definitions in fast and accurate weight optimization of truss structures is then presented. Beside the aforementioned advantages, the proposed method is very simple to implement in most metaheuristic optimization algorithms. Moreover, the method generates absolutely feasible solutions located exactly on the feasible part of the boundary of problem-specified constraints space. The method is referred to as Searching Optimum Similar Trusses (SOST). Despite of generality of the technique, its application in standard PSO is presented in this paper (PSOST). The accuracy, robustness and fast convergence rate of the proposed approach are completely investigated through optimizing several benchmark planar and spatial truss structures. The results are compared with those of standard PSO, PSOPC, HPSO and HPSACO and other algorithms wherever possible. The results show the effectiveness of this strategy in expediting the rate of convergence of optimization procedure and improving accuracy of satisfying problem-specified constraints.

## 2. Problem formulation

Weight optimization of pin-connected structures with axially loaded members involves optimizing cross sections $A_i$ of the members such that the weight of the structure $W$ is minimized and some constraints with respect to design criteria are satisfied as follows:

Minimize

$$W(A) = \sum_{k=1}^{ng} A_k \sum_{i=1}^{mk} \rho_i L_i. \tag{1}$$

Subject to:

$$\sigma_{\text{low}} \leq \sigma_i \leq \sigma_{\text{up}}, \qquad i = 1, 2, \cdots, nm, \tag{2}$$

$$\sigma_i^b \leq \sigma_i \leq 0, \qquad i = 1, 2, \cdots, ncm, \tag{3}$$

$$\delta_{\text{low}} \leq \delta_i \leq \delta_{\text{up}}, \qquad i = 1, 2, \cdots, nn, \tag{4}$$

$$A_{\text{low}} \leq A_i \leq A_{\text{up}}, \qquad i = 1, 2, \cdots, n_g, \tag{5}$$

in which $A$ is the vector containing the design variables (i.e. cross sections $A = \{A_1, A_2, \cdots, A_{ng}\}$), $W(A)$ is the weight of the truss structure, $\rho_i$ is the density of member $i$, $L_i$ is the length of member $i$, $nm$ is the number of members in the structure, $ncm$ is the number of compression members, $nn$ is the number of nodes, $ng$ is the total number of member groups (i.e. design variables), $A_k$ is the cross sectional area of the members belonging to group $k$, $mk$ is the total number of members in group $k$, $\sigma_i$ is the stress of the $i$th member, $\sigma_i^b$ is the allowable buckling stress for the $i$th member, $\delta_i$ is the displacement of the $i$th node, and *low* and *up* are the lower and upper bounds for stress, displacement and cross-sectional area.

## 3. An overview on PSO

In order to make the paper self-explanatory, a short overview on PSO algorithm is presented in this section.

The standard Particle Swarm Optimization (PSO) was first proposed by Kennedy and Eberhart [29], based on the swarm behavior such as fish and bird schooling in nature. This approach searches a space of an objective function by adjusting the trajectories of individual agents, called particles, as the piecewise path formed by positional vectors in a quasi-stochastic manner. The collection of particles is called swarm. Each particle of the swarm can be a solution of the optimization problem. The particle movement has two major components: A stochastic component and a deterministic component. The particle is attracted toward the position of the current global best, while at the same time, it has a tendency to move randomly.

When a particle finds a location that is better than any previously found locations, it updates it as

the new current best for particle $i$. There is a current best for all $n$ particles. The aim is to find the global best among all the current bests until the objective no longer improves or after a certain number of iterations is reached. In standard PSO algorithm, the swarm is updated by the following equations:

$$V_i^{k+1} = V_i^k + c_1 r_1 (P_i^k - X_i^k) + c_2 r_2 (P_g^k - X_i^k), \quad (6)$$

$$X_i^{k+1} = X_i^k + V_i^{k+1}, \quad (7)$$

where $X_i^k$ and $V_i^k$ represent the current position and the velocity of the $i$th particle at time $k$, respectively; $P_i^k$ is the best previous position of the $i$th particle (called $Pbest_i$) at time $k$, and $P_g^k$ is the best global position among all the particles in the swarm (called $gbest$) at time $k$; $r_1$ and $r_2$ are two uniform random numbers between 0 and 1.0, and $c_1$ and $c_2$ are two cognitive and social accelerating constants.

After updating the current position of particles, the new position may violate either the variables boundary constraint or problem-specified constraints boundary. Hence, the constraints of the problem should be handled accordingly.

## 4. Improved strategy

In Figure 1, the searching space in a typical constrained problem has been divided into three major regions. Region 1 forms the feasible space in which both problem-specified constraints and variables boundary constraint are satisfied. This feasible space could be a very large space in practical problems such as trusses with many members. According to Li et al. [37], for most optimization problems involving constraints, the global minimum locates on or close to the boundary of feasible design space. The main problem in finding a feasible solution which is located on the boundary of feasible space is that when particles near the boundary are moved toward the global best particles, the new position may fall outside the feasible region, and infeasible or slightly infeasible solutions are obtained. In

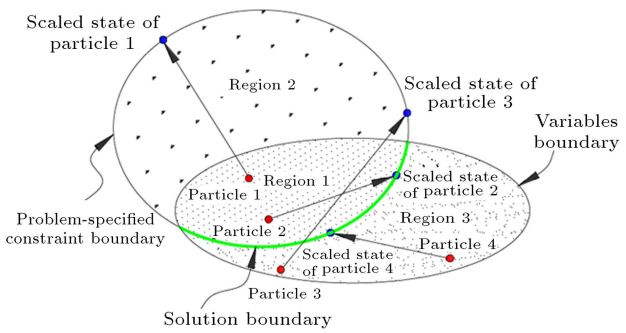


**Figure 1.** Definition of various regions in the searching space, solution boundary, particles and scaled state of particles on the boundary.

previous attempts to improve this drawback, strategies such as fly-back mechanism [35] were proposed. In this strategy, the probability of finding global optimum is increased by forcing particles which fly out of the feasible space to fly back into the region, since such particles will be likely closer to the boundary in the next iteration. Previous studies show that although the method improves handling of constraints, but in some cases slightly infeasible solutions are still obtained after fairly large number of iterations [20].

Since the optimal solution locates on the problem-specified constraint boundary and it should satisfy variables boundary at the same time, it must be located on the common part of feasible space boundary and problem-specified constraint boundary. This common part, which has been highlighted and shown in Figure 1, can be concisely called solution boundary on which the solution is sought. In large structures, the optimal solution located exactly on this boundary is very hard to achieve. The contribution of the new strategy is to rapidly find the optimal solution which is exactly located on the solution boundary.

To explain the technique, some principles of structural analysis are recalled firstly.

Under assumption of linear and elastic conditions, the following equation holds:

$$P = K.\Delta, \quad (8)$$

in which $P$ is the vector of external load, $K$ is the stiffness matrix and $\Delta$ is the vector of nodal displacements. Moreover, deformation of each bar ($\delta$) is proportional to its nodal displacements:

$$\delta \propto \Delta. \quad (9)$$

On the other hand:

$$\sigma = \frac{f}{A}, \quad (10)$$

$$f = A.\sigma = A.E\varepsilon = A.E.\frac{\delta}{L}, \quad (11)$$

in which $f$ is internal force in each bar, $\sigma$ is internal stress, $A$ is cross sectional area, $\varepsilon$ is internal strain and $L$ is the length of bar. Since the stiffness matrix is proportional to cross sectional areas, if all cross sections of a truss are multiplied by any factor $\beta$, the stiffness matrix is multiplied by the same factor $\beta$. Hence, from Eq. (8), since the external loads are constant, $\Delta$ is multiplied by $1/\beta$. From Eq. (9) it is implied that deformation is also multiplied by $1/\beta$. Consequently, Eq. (11) shows that internal force will not change, and Eq. (10) reveals that internal stress will be multiplied by factor $1/\beta$.

To employ this property, consider a hypothetical truss located on the problem-specified constraints

boundary with three bar elements shown in Figure 2(a). The upper limit of stress in bars (maximum allowable stress) is assumed to be for example $\sigma_{up} = 12$. Suppose that the cross sections are as shown on each bar element in Figure 2(a). Since the truss is located on the problem-specified constraint boundary, it has at least a member with internal stress exactly equal to $\sigma_{up} = 12$ (i.e., $\sigma_{max} = 12$ in which $\sigma_{max}$ is the maximum stress in bar elements of the truss). For the same loading, for trusses whose all cross sections are proportional to cross sections of this truss, e.g. multiplied by arbitrary factors say 0.5, 2.0 and 3.0, the maximum stresses are simply obtained by multiplying the maximum stress in the main truss by factors 2.0, 0.5 and 0.333. The maximum stress and cross sections of these new trusses are shown in Figure 2(b). Obviously, the number of trusses like those shown in Figure 2(b) is infinite.

Note that cross sectional areas of these trusses in the variables boundary can be either less or greater than cross sections of the original truss. For convenience, for the rest of this article trusses such as those shown in Figure 2(b) are called similar trusses or similar particles in the context of PSO.

**Definition 1.** For any truss located on the boundary of problem-specified constraint space, there exist infinite numbers of trusses within the variables boundary space whose all cross sectional areas are proportional to cross sectional areas of the truss. The set of these trusses are called *similar* trusses.

The term *similar* has been chosen according to the definition that a similar object is one which can be rescaled so as to coincide precisely with the other object.

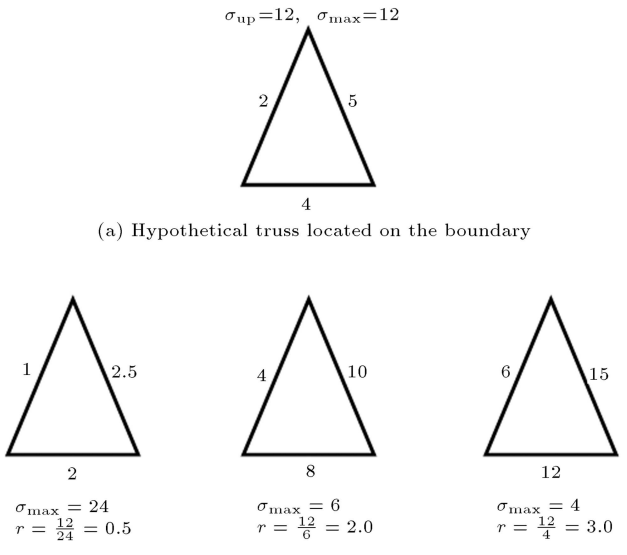


(a) Hypothetical truss located on the boundary

(b) Similar trusses (similar particles)

**Figure 2.** Definition of a truss located on the boundary of problem-specified space and similar trusses for a hypothetical 3-bars truss.

This situation can be viewed from the other side: Having any of the similar trusses such as those shown in Figure 2(b), it is possible to *scale* it to obtain cross sectional areas of the corresponding unique truss located on the problem-specified boundary in Figure 2(a). This can be achieved by the ratio $r$ defined as $r = \sigma_{up}/\sigma_{max}$, which has been shown for each similar truss in Figure 2(b). Obviously, dividing all cross sections of any similar truss by $r$ gives the cross sections of corresponding unique truss located exactly on the boundary. This permits scaling or mapping all particles to find particles located on the boundary. Although similar trusses are not optimum, they can be effectively employed in optimization procedure to remarkably expedite the rate of convergence of finding the global optimum truss, which is located on a part of problem-specified constraint boundary (i.e. solution boundary). Indeed, there are many trusses which are located on the solution boundary and the optimum one should be chosen among them. On the other hand, there are infinite numbers of trusses similar to this optimum truss in the space of variables boundary as well, which can be called *optimum similar trusses*.

**Definition 2.** For the optimum truss located on the boundary of problem-specified constraint space there exist infinite numbers of trusses within the variables boundary space whose all cross sectional areas are proportional to cross sectional areas of the optimum truss. The set of these trusses are called *optimum similar trusses*.

They are called *optimum similar trusses* since they are similar trusses associated with the optimum truss. The clever idea behind the new technique is to find one of the several optimum similar trusses having this property that when it is scaled on the solution boundary generates the best value of objective function (minimum weight). Since optimum similar trusses associated with the global optimum are infinite, the chance of finding one of optimum similar trusses is highly increased which expedites the rate of convergence of the search very significantly. No matter which optimum similar truss is found, the unique global optimum truss corresponding to each of these optimum similar trusses can be obtained by mapping (scaling) the captured optimum similar truss. This idea has been depicted in Figure 3.

When a particle (truss) is first generated in the region of variables boundary, the upper limit of allowable stress defined by the problem ($\sigma_{up}$) is already known, and the maximum stress in this truss for prescribed loading ($\sigma_{max}$) is obtained by analyzing of the truss. Therefore, the required cross sections of the truss to

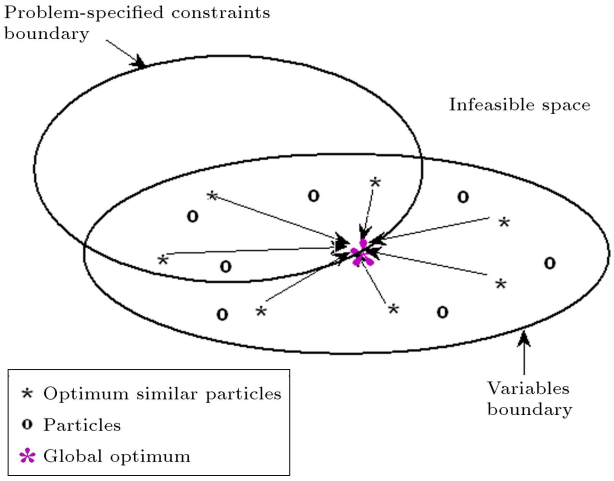


**Figure 3.** Scaling any of optimum similar trusses to obtain the optimum truss on the solution boundary.

put the particle on the problem-specified constraint boundary are obtained by scaling this particle, namely dividing all cross sectional areas of the particle by $r$. This procedure generates a *scaled* particle on the problem-specified constraint boundary (see Figure 1). However, such scaled particles may either violate or satisfy the variables boundary. In each iteration, the particle with the best fitness is selected among those scaled particles on the problem-specified boundary that satisfy the variables boundary (i.e. located on the solution boundary). The other particles are moved toward the particle whose scaled state has the best fitness, and iterations are contiued until termination criterion is met and an optimum similar truss is found. One of the main important differences between the new strategy and previous ones is that not to move all particles toward the particle which has minimum weight (global best), since such a particle generally locates near the boundary and moving particles toward this particle causes some particles to fall beyond the feasible region and become very hard to handle. It is more efficient to move all the particles toward the particle whose scaled state on the solution boundary has the minimum weight in that iteration. Then, the standard search is followed to obtain one of the optimum similar particles at the end of iterations. This completely removes difficulty in satisfying constraints and producing infeasible solutions, and results in considerable acceleration of finding optimum solution. Once the termination criterion is reached and one of the optimum similar particles associated with the global optimum is found, the global optimum can be simply obtained by scaling the optimum similar particle on the solution boundary.

Aforementioned steps for problems with single problem-specified constraint (e.g. $\sigma$) can be summarized as follows:

1. Generate population $x_i$ in the range of variables boundary;
2. Analyze each truss and find $(\sigma_{\max})_i$ for each particle;
3. Scale all particles by dividing all cross sections of $x_i$ by $r_i = \frac{\sigma_{\text{up}}}{(\sigma_{\max})_i}$ to find scaled particles $y_i$ on the boundary of problem specified constraints;
4. Check whether each component of $y_i$ violates variables boundary or not. If it does not, it is located on the solution boundary. Find fitness value of $y_i$ of such particles;
5. Find the best fitness and move all particles toward the particle whose scaled state $y_i$ has the best fitness and find new positions for $x_i$;
6. Go to next iteration until the termination condition is met;
7. One of the optimum similar particles is found. Scale it by $r$ to find the optimal solution.

Implementation of this technique in standard particle swarm optimization (PSOST) in problems with several constraints is described in pseudo-code in Table 1.

Indicating the total number of problem-specified constraints by $nc$, the swarm of particles is generated in the range of variables boundary at first. The maximum value of each constraint is determined and is denoted by $(C_j)_{\max}$. The upper limit of each constraint defined by the problem is denoted by $(C_j)_{\text{up}}$. Then, the ratio $r_j = (C_j)_{\text{up}}/(C_j)_{\max}$ is computed for each constraint, and the minimum value is selected and denoted by $r_{\min}$:

$$r_{\min} = \min(r_1, r_2, \cdots, r_j, \cdots, r_{nc}). \tag{12}$$

Then, each component of the current vector is divided by $r_{\min}$ to find the scaled state of particles on the problem-specified constraint boundary. Subsequently, the algorithm determines whether the mapped vector is on the solution boundary. If it is, it is considered for evaluating the fitness; otherwise, the previous position is kept, and the standard PSO algorithm is followed to find one of the optimum similar trusses at the end of iterations. In addition to very fast convergence, another advantage of this technique is that the solutions which absolutely satisfy problem-specified constraints are found. Contrary to the previous methods in which the solution is sought in the feasible region (region 1 in Figure 1), similar particles in this technique could be located either in region 1 or region 3. This implies that less wasted particles are generated in this new technique, which is another important advantage. Moreover, the solution found by other techniques are most of the time located near the solution boundary, whereas the current technique finds solutions exactly located on the solution boundary.

**Table 1.** The pseudo cod for PSOST.

Set $k = 1$;
Randomly initialize positions $x_i^{(k)}$ and velocities $v_i^{(k)}$ of all particles;
**WHILE** (the termination conditions are not met)
**FOR** (each particle $i$ in the swarm)
**FOR** (each specified condition of the problem $C_j$)
Calculate the ratio of allowable-to-maximum value ($r_j = c_{j_{\text{up}}}/c_{j_{\max}}$)
**END FOR**
Scale particles on the problem-specified constraint boundary:
divide each component of the current vector by minimum ratio of allowable-to-maximum value ($r_{\min}$) to find $y_i^{(k)}$
Check feasibility:
check whether each component of the mapped vector $y_i^{(k)}$ violates variables boundary or not. If it does, reset its similar particle $x_i^{(k)}$ to the previous position $x_i^{(k-1)}$
Calculate the fitness value $f(y_i^{(k)})$ of the scaled particles on the solution boundary
Update $Pbest_i$:
compare the fitness value of the $Pbest_i$ with $f(y_i^{(k)})$. If the $f(y_i^{(k)})$, is better than the fitness value of $Pbest_i$, set $Pbest_i$ to the current position $X_i^{(k)}$
Update $gbest$:
compare the fitness value of the $gbest$ with $f(y_i^{(k)})$. If the $f(y_i^{(k)})$ is better than the fitness value of $gbest$, set $gbest$ to the current position $x_i^{(k)}$
**END FOR**
Set $k = k + 1$
**FOR** (each particle $i$ in the swarm)
Generate the velocity and update the position of the current particle $x_i^{(k)}$
**END FOR**
**END WHILE**

## 5. Design examples

The efficiency and robustness of proposed PSOST are investigated through weight optimization of several planar and spatial truss structures. All truss structures considered for this research are benchmark problems which have been studied by many researchers. A computer program based on Finite Element Method (FEM) and proposed PSOST algorithm was developed to optimize the truss structures. The results obtained by this technique have been compared with those of standard PSO, PSOPC, HPSO and other methods wherever possible. In all examples, the initial swarm had 100 particles.

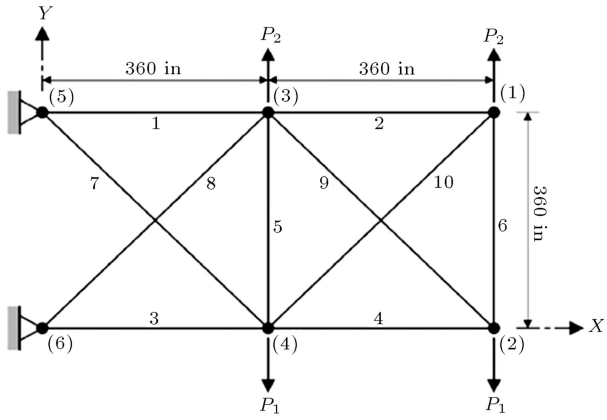


**Figure 4.** A10-bar planar truss structure.

### *5.1. 10-bar planar truss*

The planar 10-bar truss shown in Figure 4 has been used by many researchers to test the efficiency and robustness of various optimization algorithms. The material density of all members was 0.1 lb/in$^3$ and the Young's modulus of elasticity was 10,000 ksi. The maximum allowable stress in all bars was ±25 ksi with nodal displacement limitations of ±2.0 inches for both directions. The minimum cross-sectional area of each bar element was 0.1 in$^2$. The weight optimization of truss have been studied for two cases: Case 1 with $p_1 = 100$ kips and $p_2 = 0$; Case 2 with $p_1 = 150$ kips and $p_2 = 50$ kips. The variables vector consists of

ten entries corresponding to each cross-sectional area. PSOST technique was used to find the solution vector. The best solution vector was (30.53, 0.1, 23.21, 15.22, 0.1, 0.556, 7.454, 21.01, 21.54, 0.1) for Case 1 with objective function value of 5060.856 lb, and (23.54, 0.1, 25.18, 14.31, 0.1, 1.97, 12.41, 12.86, 20.39, 0.1) for Case 2 with objective function value of 4676.963 lb. Tables 2 and 3 report the best and the worst solution vector for Cases 1 and 2, respectively. In these tables, the solutions obtained by standard PSO [37], PSOPC [37], HPSO [37], HS [16], HPSACO [41], EHS [20], SAHS [20], and the study carried out by Sedaghati [42], Farshi and Alinia-ziazi [43] and Schmit and Farshi [44] are reported as well. Analysis of structures with the cross sections found by PSOST given in Tables 2 and 3 shows that in both cases the solutions found by PSOST are exactly located on the solution boundary (i.e. $\sigma_{\max} = \sigma_{\text{up}}$ and $\delta_{\max} = \delta_{\text{up}}$). For this particular problem, both constraints are simultaneously located on the boundary. However, for

**Table 2.** Comparison of optimal design for the 10-bar planar truss structure (Case 1).

| Variables | | Optimal cross-sectional areas (in.$^2$) | | | | | | | | | | |
|---|---|---|---|---|---|---|---|---|---|---|---|---|
| | | Lee and Geem [16] | Sedaghati [42] | Kaveh and Talatahari [41] | Farshi and Alinia-ziazi [43] | Li et al. [37] | | | Degertekin [20] | | This study | |
| | | HS | | HPSACO | | PSO | PSOPC | HPSO | EHS | SAHS | $\text{PSOST}_{\text{best}}$ | $\text{PSOST}_{\text{worst}}$ |
| 1 | $A_1$ | 30.15 | 30.5218 | 30.307 | 30.5208 | 33.469 | 30.569 | 30.704 | 30.208 | 30.394 | 30.53135 | 30.57354 |
| 2 | $A_2$ | 0.102 | 0.1000 | 0.100 | 0.1000 | 0.110 | 0.100 | 0.100 | 0.100 | 0.100 | 0.10000 | 0.10001 |
| 3 | $A_3$ | 22.71 | 23.1999 | 23.434 | 23.2040 | 23.177 | 22.974 | 23.167 | 22.698 | 23.098 | 23.21091 | 23.07489 |
| 4 | $A_4$ | 15.27 | 15.2229 | 15.505 | 15.2232 | 15.475 | 15.148 | 15.183 | 15.275 | 15.491 | 15.21851 | 15.31845 |
| 5 | $A_5$ | 0.102 | 0.100 | 0.100 | 0.1000 | 3.649 | 0.100 | 0.100 | 0.100 | 0.100 | 0.10000 | 0.10001 |
| 6 | $A_6$ | 0.544 | 0.5514 | 0.5241 | 0.5515 | 0.116 | 0.547 | 0.551 | 0.529 | 0.529 | 0.555815 | 0.53916 |
| 7 | $A_7$ | 7.541 | 7.4572 | 7.4365 | 7.4669 | 8.328 | 7.493 | 7.460 | 7.558 | 7.488 | 7.454248 | 7.48932 |
| 8 | $A_8$ | 21.56 | 21.0364 | 21.079 | 21.0342 | 23.340 | 21.159 | 20.978 | 21.559 | 21.189 | 21.01724 | 21.18769 |
| 9 | $A_9$ | 21.45 | 21.5284 | 21.229 | 21.5294 | 23.014 | 21.556 | 21.508 | 21.491 | 21.342 | 21.53604 | 21.34198 |
| 10 | $A_{10}$ | 0.100 | 0.1000 | 0.100 | 0.1000 | 0.190 | 0.100 | 0.100 | 0.100 | 0.100 | 0.10000 | 0.10000 |
| Weight (lb) | | 5057.88 | 5060.85 | 5056.56 | 5061.4 | 5529.50 | 5061.00 | 5060.92 | 5062.39 | 5061.42 | 5060.856 | 5061.061 |
| Number of structural analyses | | 15000 | N/A | 9925 | N/A | 150000 | 150000 | 125000 | 11402 | 7267 | 5900 | 5400 |

**Table 3.** Comparison of optimal design for the 10-bar planar truss structure (Case 2).

| Variables | | Optimal cross-sectional areas (in.$^2$) | | | | | | | | | | |
|---|---|---|---|---|---|---|---|---|---|---|---|---|
| | | Lee and Geem [16] | Schmit and Farshi [44] | Kaveh and Talatahari [41] | Farshi and Alinia-ziazi [43] | Li et al. [37] | | | Degertekin [20] | | This study | |
| | | HS | | HPSACO | | PSO | PSOPC | HPSO | EHS | SAHS | $\text{PSOST}_{\text{best}}$ | $\text{PSOST}_{\text{worst}}$ |
| 1 | $A_1$ | 23.25 | 24.29 | 23.194 | 23.5270 | 22.935 | 23.743 | 23.353 | 23.589 | 23.525 | 23.53781 | 23.75450 |
| 2 | $A_2$ | 0.102 | 0.100 | 0.100 | 0.1000 | 0.113 | 0.101 | 0.100 | 0.100 | 0.100 | 0.10000 | 0.10015 |
| 3 | $A_3$ | 25.73 | 23.35 | 24.585 | 25.2941 | 25.355 | 25.287 | 25.502 | 25.422 | 25.429 | 25.18370 | 24.92136 |
| 4 | $A_4$ | 14.51 | 13.66 | 14.221 | 14.3760 | 14.373 | 14.413 | 14.250 | 14.488 | 14.488 | 14.30917 | 14.10767 |
| 5 | $A_5$ | 0.100 | 0.100 | 0.100 | 0.1000 | 0.100 | 0.100 | 0.100 | 0.100 | 0.100 | 0.10000 | 0.10007 |
| 6 | $A_6$ | 1.977 | 1.969 | 1.969 | 1.9698 | 1.990 | 1.969 | 1.972 | 1.975 | 1.992 | 1.96972 | 1.98002 |
| 7 | $A_7$ | 12.21 | 12.67 | 12.489 | 12.4041 | 12.346 | 12.362 | 12.363 | 12.362 | 12.352 | 12.41567 | 12.46655 |
| 8 | $A_8$ | 12.61 | 12.54 | 12.925 | 12.8245 | 12.923 | 12.694 | 12.894 | 12.682 | 12.698 | 12.85672 | 12.83668 |
| 9 | $A_9$ | 20.36 | 21.97 | 20.952 | 20.3304 | 20.678 | 20.323 | 20.356 | 20.322 | 20.341 | 20.38820 | 20.55069 |
| 10 | $A_{10}$ | 0.100 | 0.100 | 0.101 | 0.1000 | 0.100 | 0.103 | 0.101 | 0.100 | 0.100 | 0.10000 | 0.10319 |
| Weight (lb) | | 4668.81 | 4691.84 | 4675.78 | 4677.8 | 4679.47 | 4677.70 | 4677.29 | 4679.02 | 4678.84 | 4676.963 | 4678.450 |
| Number of structural analyses | | 15000 | N/A | 9925 | N/A | 150000 | 150000 | 125000 | 11402 | 7267 | 6200 | 5800 |

some problems, one of these constraints is influential and controls the design.

It is worth pointing out that the structures obtained by the other methods which violate the design constraints may be lighter structures. However, design is very sensitive to amount of constraint violation. Therefore, to make the comparison meaningful, the results of current study should be compared with those methods that generate absolutely feasible solutions same as PSOST.

As Table 2 shows, compared to PSO, PSOPC, HPSO, EHS and the solution found by Farshi and Alinia-ziazi, PSOST gives better result similar to Sedaghati's study but with different cross sections. Moreover, there is no significant difference between the best and worst solutions obtained by PSOST, which is another positive aspect of the present technique.

As Table 3 indicates, compared to PSO, EHS, SAHS, and the solution found by Farshi and Alinia-ziazi, PSOST gives a lighter structure with the weight of 4676.963 lb.

Considering the number of structural analyses required for each technique in Tables 2 and 3, PSOST is the most computationally effective algorithm requiring 5900 and 6200 analyses for Cases 1 and 2, respectively.

Taking the rate of convergence into account, it should be noted that standard PSO converges after approximately 2800 and 2100 iterations for Cases 1 and 2, respectively; PSOPC converges after approximately 1250 and 1000 iterations for Cases 1 and 2, respectively; and HPSO converges after approximately 800 and 900 iterations for Cases 1 and 2, respectively. The current technique finds the best solution vector with approximately 70 iterations for both cases, which shows very considerable improvement in expediting the rate of convergence. Figures 5 and 6 compare the convergence rate of PSOST and three other algorithms for Cases 1 and 2, respectively. As the figures show, the current method finds good solutions even in the early iterations.

To explore the robustness and stability of the new technique and to show the independence of the solution on the initial swarm, convergence rates of 5 independent runs of PSOST for Case 1 of this problem have been depicted in Figure 7, which show the same trends.

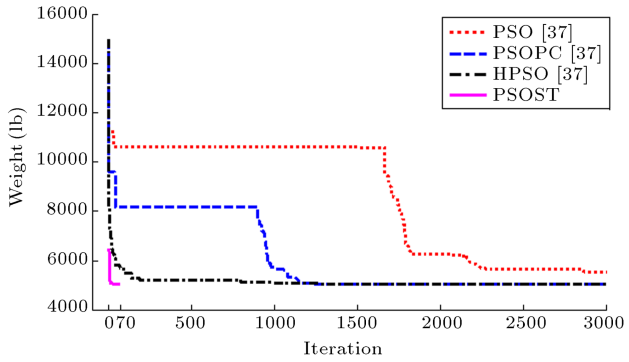


**Figure 5.** Comparison of the convergence rates of four algorithms for the 10-bar planar truss structure (Case 1).

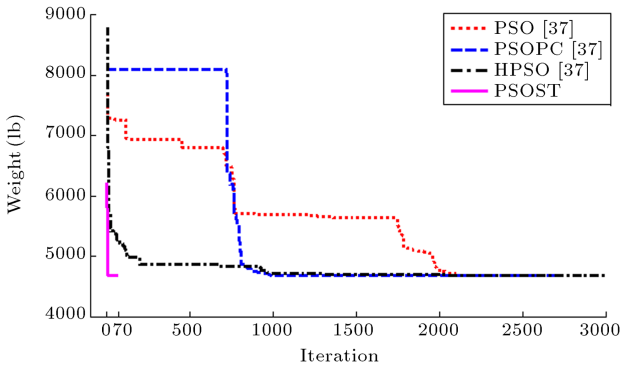


**Figure 6.** Comparison of the convergence rates of four algorithms for the 10-bar planar truss structure (Case 2).

### *5.2. 25-bar spatial truss*

Figure 8 shows the well-known 25-bar spatial truss in which modulus of elasticity of the material was 10,000 ksi and its density was 0.1 lb/in$^3$. Table 4 reports the two load cases examined for this example. The design variables of the structure and the allowable stress values for all groups are listed in Table 5. All nodes in all directions are subjected to the displacement limits of ±0.35 in. Moreover, the minimum cross-sectional area for each group of elements was 0.01 in$^2$.

Table 6 reports optimization results obtained for 25-bar truss from this study and the results obtained

**Table 4.** Load cases for the 25-bar spatial truss structure.

| Node | Case 1 (Kips) | | | Case 2 (Kips) | | |
|---|---|---|---|---|---|---|
| | $P_x$ | $P_y$ | $P_z$ | $P_x$ | $P_y$ | $P_z$ |
| 1 | 0.0 | 20.0 | -5.0 | 1.0 | 10.0 | -5.0 |
| 2 | 0.0 | -20.0 | -5.0 | 0.0 | 10.0 | -5.0 |
| 3 | 0.0 | 0.0 | 0.0 | 0.5 | 0.0 | 0.0 |
| 6 | 0.0 | 0.0 | 0.0 | 0.5 | 0.0 | 0.0 |

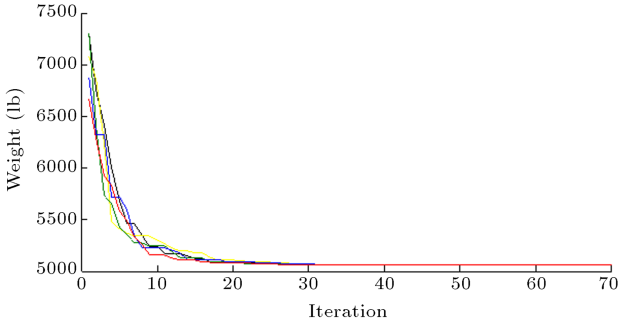


**Figure 7.** Comparison of the convergence rates of five independent runs of PSOST algorithm for the 10-bar planar truss structure (Case 1).

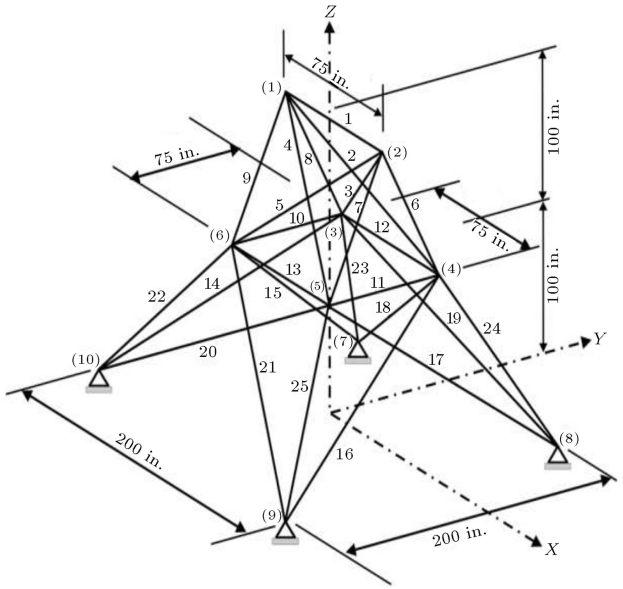


**Figure 8.** A25-bar spatial truss structure.

**Table 5.** Member stress limits for the 25-bar spatial truss structure.

| | Variables | Compressive stress limitations (ksi) | Tensile stress limitations (ksi) |
|---|---|---|---|
| 1 | $A_1$ | 35.092 | 40.0 |
| 2 | $A_2 \sim A_5$ | 11.590 | 40.0 |
| 3 | $A_6 \sim A_9$ | 17.305 | 40.0 |
| 4 | $A_{10} \sim A_{11}$ | 35.092 | 40.0 |
| 5 | $A_{12} \sim A_{13}$ | 35.092 | 40.0 |
| 6 | $A_{14} \sim A_{17}$ | 6.759 | 40.0 |
| 7 | $A_{18} \sim A_{21}$ | 6.959 | 40.0 |
| 8 | $A_{22} \sim A_{25}$ | 11.802 | 40.0 |

by other researches. The structural analyses show that the influential parameter in optimum design of this structure is the allowable compressive stress in group 8 of cross sections which must not exceed -6.959 ksi specified by the problem (in Table 5). Analyzing the structure with the cross sectional areas found by PSOST, reported in Table 6, reveals that the solution obtained by PSOST is located exactly on the solution boundary, contrary to the other solutions. That is, for the solution found by PSOST, the value of compressive stress in elements 18 and 19 in load Case 1 one of the members of group 8 is exactly -6.959 ksi in load Case 2 and absolute displacement in nodes 1 and 2 in Y direction are 0.35 in in both load cases. The value of the objective function achieved by PSOST was 545.167 lb after a few numbers of structural analyses equal to 6400. Compared to PSO, HPSO and EHS, the solution found by the current algorithm gives the best absolutely feasible solution.

Figure 9 compares the convergence rate of PSOST with PSO, PSOPC and HPSO. As it is clear from Figure 9, PSOST leads to a much better solution in the early iterations and converges rapidly. Figure 10 compares the rate of convergence of 5 independent runs of PSOST for this example, and the trends are the same.

### *5.3. 72-bar spatial truss*

The third problem is weight optimization of 72-bar spatial truss structure shown in Figure 11 The modulus of elasticity of the material was 10,000 ksi and material density was 0.1 lb/in$^3$. The cross-sectional areas of members as design variables are separated into 16 groups:

**Table 6.** Comparison of optimal design for the 25-bar spatial truss structure.

| | Variables | Optimal cross-sectional areas (in.$^2$) | | | | | | | | | | |
|---|---|---|---|---|---|---|---|---|---|---|---|---|
| | | Lee and Geem [16] HS | Farshi and Alinia-ziazi [43] | Kaveh and Talatahari [41] HPSACO | Camp [25] | Li et al. [37] PSO | Li et al. [37] PSOPC | Li et al. [37] HPSO | Degertekin [20] EHS | Degertekin [20] SAHS | This study $PSOST_{best}$ | This study $PSOST_{worst}$ |
| 1 | $A_1$ | 0.047 | 0.0100 | 0.010 | 0.010 | 9.863 | 0.010 | 0.010 | 0.010 | 0.010 | 0.01000 | 0.01195 |
| 2 | $A_2 \sim A_5$ | 2.022 | 1.9981 | 2.054 | 2.092 | 1.798 | 1.979 | 1.970 | 1.995 | 2.074 | 1.99935 | 2.03857 |
| 3 | $A_6 \sim A_9$ | 2.950 | 2.9828 | 3.008 | 2.964 | 3.654 | 3.011 | 3.016 | 2.980 | 2.961 | 2.97514 | 2.91835 |
| 4 | $A_{10} \sim A_{11}$ | 0.010 | 0.0100 | 0.010 | 0.010 | 0.100 | 0.010 | 0.010 | 0.010 | 0.010 | 0.01000 | 0.01060 |
| 5 | $A_{12} \sim A_{13}$ | 0.014 | 0.0100 | 0.010 | 0.010 | 0.100 | 0.010 | 0.010 | 0.010 | 0.010 | 0.01000 | 0.01000 |
| 6 | $A_{14} \sim A_{17}$ | 0.688 | 0.6837 | 0.679 | 0.689 | 0.596 | 0.657 | 0.694 | 0.696 | 0.691 | 0.68358 | 0.68615 |
| 7 | $A_{18} \sim A_{21}$ | 1.657 | 1.6750 | 1.611 | 1.601 | 1.659 | 1.678 | 1.681 | 1.679 | 1.617 | 1.67501 | 1.66893 |
| 8 | $A_{22} \sim A_{25}$ | 2.663 | 2.6668 | 2.678 | 2.686 | 2.612 | 2.693 | 2.643 | 2.652 | 2.674 | 2.66794 | 2.68105 |
| Weight (lb) | | 544.38 | 545.37 | 544.99 | 545.38 | 629.08 | 545.27 | 545.19 | 545.49 | 545.12 | 545.167 | 545.258 |
| Number of structural analyses | | 15000 | N/A | 9875 | 20566 | 150000 | 150000 | 125000 | 10391 | 9051 | 6400 | 6900 |

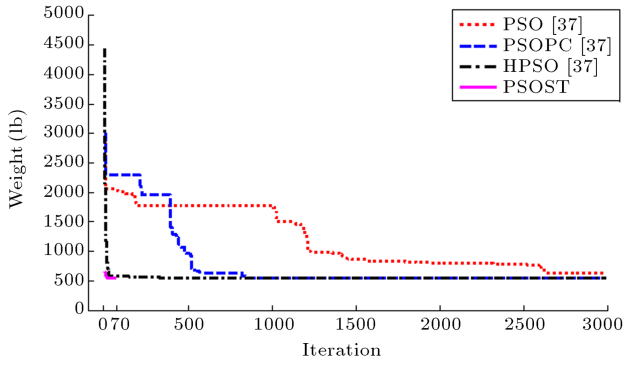


**Figure 9.** Comparison of the convergence rates of four algorithms for the 25-bar spatial truss structure.

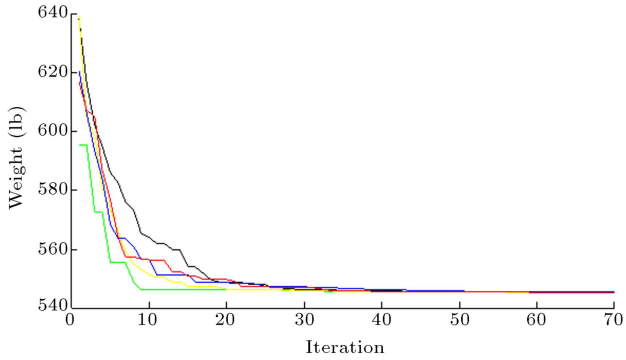


**Figure 10.** Comparison of the convergence rates of five independent runs of PSOST algorithm for the 25-bar spatial truss structure.

(1) A1-A4, (2) A5-A12, (3) A13-A16,
(4) A17-A18, (5) A19-A22, (6) A23-A30,
(7) A31-A34, (8) A35-A36, (9) A37-A40,
(10) A41-A48, (11) A49-A52, (12) A53-A54,
(13) A55-A58, (14) A59-A66, (15) A67-A70,
(16) A71-A72.

The maximum allowable stress in all members was equal in tension and compression, and it was ±25 ksi. Maximum allowable displacement of uppermost nodes was ±0.25 inches in both $x$ and $y$ directions. Table 7 reports the two load cases for this example. This problem was analyzed for two cases: Case 1 in which minimum cross-sectional area of each members was 0.1 $in^2$, and Case 2 in which this value was 0.01 $in^2$.

**Table 7.** Load cases for the 72-bar spatial truss structure.

| Node | Case 1 (Kips) | | | Case 2 (Kips) | | |
|---|---|---|---|---|---|---|
| | $P_x$ | $P_y$ | $P_z$ | $P_x$ | $P_y$ | $P_z$ |
| 17 | 5.0 | 5.0 | -5.0 | 0.0 | 0.0 | -5.0 |
| 18 | 0.0 | 0.0 | 0.0 | 0.0 | 0.0 | -5.0 |
| 19 | 0.0 | 0.0 | 0.0 | 0.0 | 0.0 | -5.0 |
| 20 | 0.0 | 0.0 | 0.0 | 0.0 | 0.0 | -5.0 |

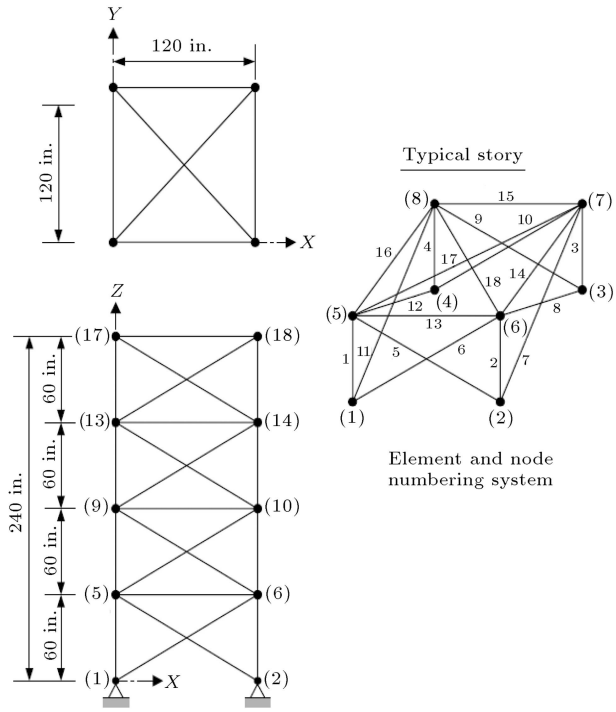


**Figure 11.** A 72-bar spatial truss structure.

After 6500 and 5900 structural analyses, PSOST algorithm finds the best cross sections shown in Tables 8 and 9 for Cases 1 and 2, respectively. These tables also compare the optimization results of this study with those of other references. The value of objective function found by PSOST was 379.618 lb for Case 1 and 363.824 lb for Case 2.

For Case 1, the solutions found by Perez and Behdinan [36], Kaveh and Talatahari [26], Camp [25], EHS algorithm of Degertekin [20] and current study (PSOST) are absolutely feasible. As it is clear from Table 8, the structure found by PSOST is the lightest structure among the aforementioned structures. For Case 2, among the methods presented in Table 9, simple GA, PSOPC, EHS, SAHS and PSOST give absolutely feasible solutions. Table 9 shows that the solution found by PSOST is the best solution among the aforementioned methods in this case as well. Moreover, the solutions obtained by PSOST in both cases are exactly located on the solution boundary and to the authors' knowledge, they are the only solutions reported in the literature with this property up to now. Figure 12 compares the rate of convergence of the present technique with PSO, PSOPC and HPSO for Case 2. As the figure indicates, the rate of convergence of PSOST is much better. Figure 13 compares the rate of convergence of five independent runs by PSOST for Case 1 of this problem.

The capability of current technique in solving more complex problems is investigated through the following two last examples.

**Table 8.** Comparison of optimal design for the 72-bar spatial truss structure (Case 1).

| Variables | Optimal cross-sectional areas (in.$^2$) | | | | | | | |
|---|---|---|---|---|---|---|---|---|
| | Lee and Geem [16] | Perez and Behdinan [36] | Kaveh and Talatahari [26] | Camp [25] | Degertekin [20] | | This study | |
| | HS | PSO | HBB-BC | BB-BC | EHS | SAHS | PSOST$_{best}$ | PSOST$_{worst}$ |
| 1 $A_1 \sim A_4$ | 1.7901 | 1.7427 | 1.9042 | 1.8577 | 1.967 | 1.860 | 1.884893 | 1.865121 |
| 2 $A_5 \sim A_{12}$ | 0.521 | 0.5185 | 0.5162 | 0.5059 | 0.510 | 0.521 | 0.511212 | 0.509557 |
| 3 $A_{13} \sim A_{16}$ | 0.100 | 0.1000 | 0.1000 | 0.1000 | 0.100 | 0.100 | 0.100000 | 0.100006 |
| 4 $A_{17} \sim A_{18}$ | 0.100 | 0.1000 | 0.1000 | 0.1000 | 0.100 | 0.100 | 0.100000 | 0.100053 |
| 5 $A_{19} \sim A_{22}$ | 1.229 | 1.3079 | 1.2582 | 1.2476 | 1.293 | 1.271 | 1.273314 | 1.260573 |
| 6 $A_{23} \sim A_{30}$ | 0.522 | 0.5193 | 0.5035 | 0.5269 | 0.511 | 0.509 | 0.509822 | 0.507924 |
| 7 $A_{31} \sim A_{34}$ | 0.100 | 0.1000 | 0.1000 | 0.1000 | 0.100 | 0.100 | 0.100000 | 0.100015 |
| 8 $A_{35} \sim A_{36}$ | 0.100 | 0.1000 | 0.1000 | 0.1012 | 0.100 | 0.100 | 0.100000 | 0.10203 |
| 9 $A_{37} \sim A_{40}$ | 0.517 | 0.5142 | 0.5178 | 0.5209 | 0.499 | 0.485 | 0.525298 | 0.535832 |
| 10 $A_{41} \sim A_{48}$ | 0.504 | 0.5464 | 0.5214 | 0.5172 | 0.501 | 0.501 | 0.516069 | 0.526008 |
| 11 $A_{49} \sim A_{52}$ | 0.100 | 0.1000 | 0.1000 | 0.1004 | 0.100 | 0.100 | 0.100000 | 0.100073 |
| 12 $A_{53} \sim A_{54}$ | 0.101 | 0.1095 | 0.1007 | 0.1005 | 0.100 | 0.100 | 0.100000 | 0.125054 |
| 13 $A_{55} \sim A_{58}$ | 0.156 | 0.1615 | 0.1566 | 0.1565 | 0.160 | 0.168 | 0.156347 | 0.154919 |
| 14 $A_{59} \sim A_{66}$ | 0.547 | 0.5092 | 0.5421 | 0.5507 | 0.522 | 0.584 | 0.547823 | 0.548436 |
| 15 $A_{67} \sim A_{70}$ | 0.442 | 0.4967 | 0.4132 | 0.3922 | 0.478 | 0.433 | 0.411418 | 0.400562 |
| 16 $A_{71} \sim A_{72}$ | 0.590 | 0.5619 | 0.5756 | 0.5922 | 0.591 | 0.520 | 0.570194 | 0.563949 |
| Weight (lb) | 379.27 | 381.91 | 379.66 | 379.85 | 381.03 | 380.62 | 379.618 | 380.000 |
| Number of structural analyses | 20000 | N/A | 13200 | 19621 | 15044 | 13742 | 6500 | 6100 |

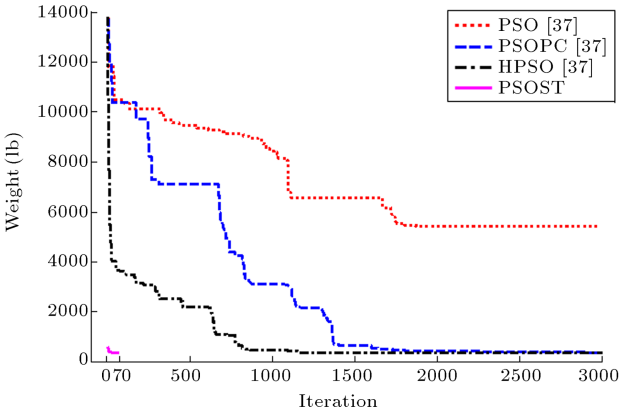


**Figure 12.** Comparison of the convergence rates of four algorithms for the 72-bar spatial truss structure (Case 2).

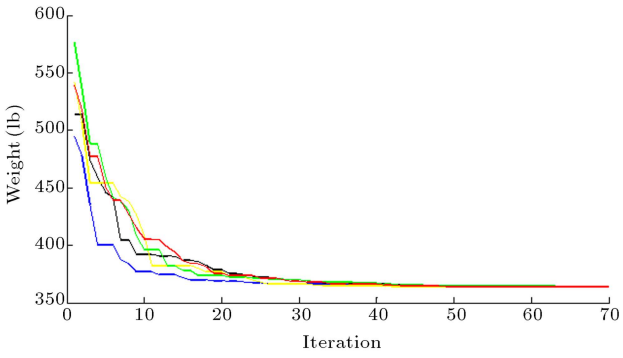


**Figure 13.** Comparison of the convergence rates of five independent runs of PSOST algorithm for the 72-bar spatial truss structure (Case 1).

### *5.4. 200-bar planar truss*

The 200-bar planar truss depicted in Figure 14 has been widely studied by researchers [16,20,41]. The Young's modulus of elasticity of the material was 30,000 ksi and material density was 0.283 lb/in$^3$. There were no constraints for displacements, but the maximum allowable stresses in tension and compression were both equal to 10 ksi. The cross-sectional areas of members were divided into 29 groups as shown in Table 10.

The structure was imposed to the following loading conditions:

1. Horizontal loads equal to 10 kips acting at nodes 1, 6, 15, 20, 29, 34, 43, 48, 57, 62 and 71 in positive $x$-direction.

**Table 9.** Comparison of optimal design for the 72-bar spatial truss structure (Case 2).

| Variables | Optimal cross-sectional areas (in.$^2$) | | | | | | | | | | |
|---|---|---|---|---|---|---|---|---|---|---|---|
| | Lee and Geem [16] | Lamberti [18] | Sarma [6] | | Li et al. [37] | | | Degertekin [20] | | This study | |
| | HS | CMLPSA | Simple GA | Fuzzy GA | PSO | PSOPC | HPSO | EHS | SAHS | $PSOST_{best}$ | $PSOST_{worst}$ |
| 1 $A_1 \sim A_4$ | 1.963 | 1.8866 | 2.141 | 1.732 | 40.053 | 1.652 | 1.907 | 1.889 | 1.889 | 1.88635 | 1.90401 |
| 2 $A_5 \sim A_{12}$ | 0.481 | 0.5169 | 0.510 | 0.522 | 0.237 | 0.547 | 0.524 | 0.502 | 0.520 | 0.51701 | 0.52989 |
| 3 $A_{13} \sim A_{16}$ | 0.010 | 0.0100 | 0.054 | 0.010 | 21.692 | 0.100 | 0.010 | 0.010 | 0.010 | 0.01000 | 0.01037 |
| 4 $A_{17} \sim A_{18}$ | 0.011 | 0.0100 | 0.010 | 0.013 | 0.657 | 0.101 | 0.010 | 0.010 | 0.010 | 0.01000 | 0.01001 |
| 5 $A_{19} \sim A_{22}$ | 1.233 | 1.2903 | 1.489 | 1.345 | 22.144 | 1.102 | 1.288 | 1.284 | 1.289 | 1.28957 | 1.28552 |
| 6 $A_{23} \sim A_{30}$ | 0.506 | 0.5170 | 0.551 | 0.551 | 0.266 | 0.589 | 0.523 | 0.526 | 0.524 | 0.51658 | 0.51682 |
| 7 $A_{31} \sim A_{34}$ | 0.011 | 0.0100 | 0.057 | 0.010 | 1.654 | 0.011 | 0.010 | 0.010 | 0.010 | 0.01000 | 0.01000 |
| 8 $A_{35} \sim A_{36}$ | 0.012 | 0.0100 | 0.013 | 0.013 | 10.284 | 0.010 | 0.010 | 0.010 | 0.010 | 0.01000 | 0.01003 |
| 9 $A_{37} \sim A_{40}$ | 0.538 | 0.5207 | 0.565 | 0.492 | 0.559 | 0.581 | 0.544 | 0.528 | 0.539 | 0.52047 | 0.52764 |
| 10 $A_{41} \sim A_{48}$ | 0.533 | 0.5180 | 0.527 | 0.545 | 12.883 | 0.458 | 0.528 | 0.525 | 0.519 | 0.51841 | 0.52330 |
| 11 $A_{49} \sim A_{52}$ | 0.010 | 0.0100 | 0.010 | 0.066 | 0.138 | 0.010 | 0.019 | 0.010 | 0.015 | 0.01000 | 0.03918 |
| 12 $A_{53} \sim A_{54}$ | 0.167 | 0.1141 | 0.066 | 0.013 | 0.188 | 0.152 | 0.020 | 0.063 | 0.105 | 0.11359 | 0.06304 |
| 13 $A_{55} \sim A_{58}$ | 0.161 | 0.1665 | 0.174 | 0.178 | 29.048 | 0.161 | 0.176 | 0.173 | 0.167 | 0.16652 | 0.16762 |
| 14 $A_{59} \sim A_{66}$ | 0.542 | 0.5363 | 0.425 | 0.524 | 0.632 | 0.555 | 0.535 | 0.550 | 0.532 | 0.53635 | 0.52650 |
| 15 $A_{67} \sim A_{70}$ | 0.478 | 0.4460 | 0.437 | 0.396 | 3.045 | 0.514 | 0.426 | 0.444 | 0.425 | 0.44549 | 0.42113 |
| 16 $A_{71} \sim A_{72}$ | 0.551 | 0.5761 | 0.641 | 0.595 | 1.711 | 0.648 | 0zcc.612 | 0.592 | 0.579 | 0.57778 | 0.60363 |
| Weight (lb) | 364.33 | 363.818 | 372.40 | 364.40 | 5417.02 | 368.45 | 364.86 | 364.36 | 364.05 | 363.824 | 364.646 |
| Number of structural analyses | 20000 | 900 | N/A | N/A | 150000 | 125000 | 125000 | 13755 | 12852 | 5900 | 6000 |

**Table 10.** Design variable for the 200-bar planar truss structure.

| Design variables | Member number | Design variables | Member number |
|---|---|---|---|
| 1 | 1,2,3,4 | 16 | 82,83,85,86,88,89,91,92,103,104,106,107, 109,110,112,113 |
| 2 | 5,8,11,14,17 | 17 | 115,116,117,118 |
| 3 | 19,20,21,22,23,24 | 18 | 119,122,125,128,131 |
| 4 | 18,25,56,63,94,101,132,139,170,177 | 19 | 133,134,135,136,137,138 |
| 5 | 26,29,32,35,38 | 20 | 140,143,146,149,152 |
| 6 | 6,7,9,10,12,13,15,16,27,28,30,31,33, 34,36,37 | 21 | 120,121,123,124,126,127,129,130, 141,142,144,145,147,148,150,151 |
| 7 | 39,40,41,42 | 22 | 153,154,155,156 |
| 8 | 43,46,49,52,55 | 23 | 157,160,163,166,169 |
| 9 | 57,58,59,60,61,62 | 24 | 171,172,173,174,175,176 |
| 10 | 64,67,70,73,76 | 25 | 178,181,184,187,190 |
| 11 | 44,45,47,48,50,51,53,54,65,66, 68,69,71,72,74,75 | 26 | 158,159,161,162,164,165,167,168,179, 180,182,183,185,186,188,189 |
| 12 | 77,78,79,80 | 27 | 191,192,193,194 |
| 13 | 81,84,87,90,93 | 28 | 195,197,198,200 |
| 14 | 95,96,97,98,99,100 | 29 | 196,199 |
| 15 | 102,105,108,111,114 | | |

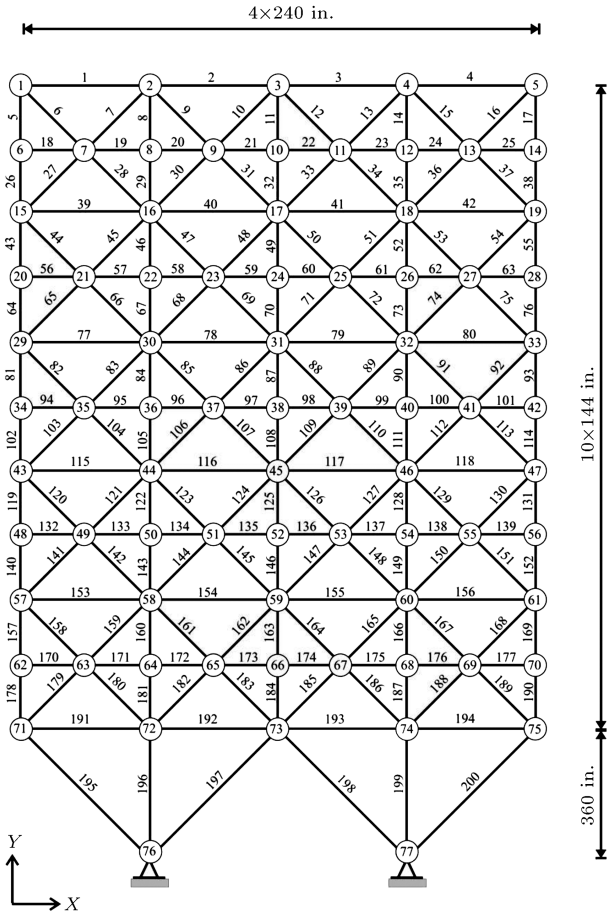


**Figure 14.** A 200-bar planar truss structure.

2. Vertical downward loads equal to 10 kips acting at nodes 1, 2, 3, 4, 5, 6, 8, 10, 12, 14, 15, 16, 17, 18, 19, 20, 22, 24, 26, 28, 29, 30, 31, 32, 33, 34, 36, 38, 40, 42, 43, 44, 45, 46, 47, 48, 50, 52, 54, 56, 57, 58, 59, 60, 61, 62, 64, 66, 68, 70, 71, 72, 73, 74, and 75.
3. Loading conditions (1) and (2) acting simultaneously.

Table 11 compares the optimum results obtained by PSOST and other studies. The value of the objective function found by PSOST is 25519.03. Compared to absolutely feasible solutions obtained by EHS and SAHS, the absolutely feasible solution found by PSOST is a lighter structure than the solution found by EHS and it is heavier than the solution found by SAHS. It is worthy of remark that the better solution obtained by SAHS is also located exactly on the solution boundary same as the solution found by PSOST. It leads to this interesting consequence that SOST technique can be combined with more sophisticated searching algorithms to obtain even better results.

However, taking the computational effort into account, PSOST needs 9700 analyses, very less than 22851 analyses required for EHS and 19670 analyses required for SAHS. In Figure 15 the rates of convergence of various methods are compared.

### *5.5. 120-bar spatial truss*

The final test is devoted to 120-bar dome truss depicted in Figure 16. The optimization of this truss structure is complicated, owing to specific design criteria. Hence, this spatial truss has been analyzed by few researches such as Lee and Geem [16] and Kaveh and Talatahari [41]. The previous studies revealed that standard PSO was unable to find the optimum cross-sectional areas even after a fairly large number of iterations [41]. Allowable tensile and compressive stresses are considered according to AISC ASD (1989) [45] code

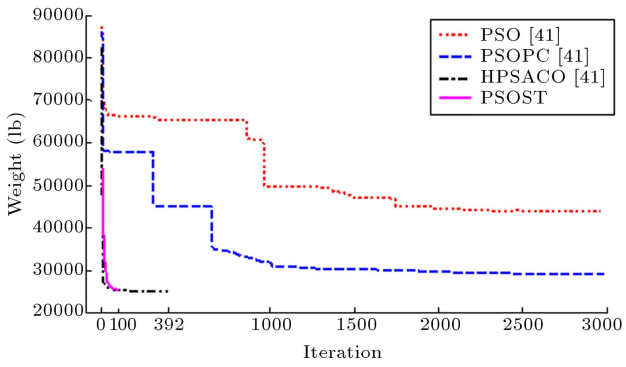


**Figure 15.** Comparison of the convergence rates of four algorithms for the 200-bar planar truss structure.

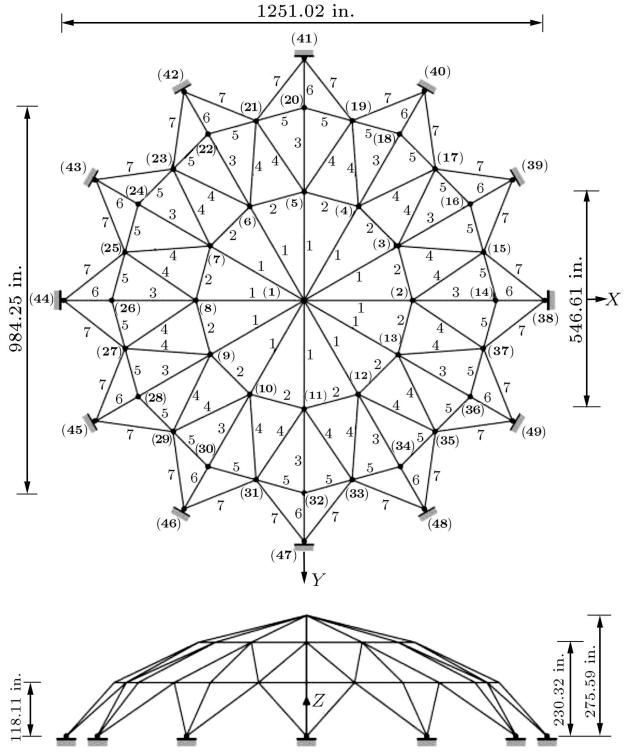


**Figure 16.** A 120-bar spatial truss structure.

**Table 11.** Comparison of optimal design for the 200-bar planar truss structure.

| Design variables | Optimal cross-sectional areas (in.$^2$) | | | | | | | |
|---|---|---|---|---|---|---|---|---|
| | Lee and Geem [16] | Degertekin [20] | | Kaveh and Talatahari [41] | | | This study | |
| | HS | EHS | SAHS | PSO | PSOPC | HPSACO | $PSOST_{best}$ | $PSOST_{worst}$ |
| 1 | 0.1253 | 0.150 | 0.154 | 0.8016 | 0.7590 | 0.1033 | 0.13347 | 0.17053 |
| 2 | 1.0157 | 0.946 | 0.941 | 2.4028 | 0.9032 | 0.9184 | 0.94066 | 1.67457 |
| 3 | 0.1069 | 0.101 | 0.100 | 4.3407 | 1.1000 | 0.1202 | 0.10000 | 0.29653 |
| 4 | 0.1096 | 0.100 | 0.100 | 5.6972 | 0.9952 | 0.1009 | 0.10000 | 0.13957 |
| 5 | 1.9369 | 1.945 | 1.942 | 3.9538 | 2.1350 | 1.8664 | 1.94066 | 2.45534 |
| 6 | 0.2686 | 0.296 | 0.301 | 0.5950 | 0.4193 | 0.2826 | 0.29262 | 0.43543 |
| 7 | 0.1042 | 0.100 | 0.100 | 5.6080 | 1.0041 | 0.1000 | 0.18899 | 0.20751 |
| 8 | 2.9731 | 3.161 | 3.108 | 9.1953 | 2.8052 | 2.9683 | 3.11294 | 3.10808 |
| 9 | 0.1309 | 0.102 | 0.100 | 4.5128 | 1.0344 | 0.1000 | 0.10000 | 0.16364 |
| 10 | 4.1831 | 4.199 | 4.106 | 4.6012 | 3.7842 | 3.9456 | 4.11294 | 4.06041 |
| 11 | 0.3967 | 0.401 | 0.409 | 0.5552 | 0.5269 | 0.3742 | 0.44074 | 0.45693 |
| 12 | 0.4416 | 0.181 | 0.191 | 18.7510 | 0.4302 | 0.4501 | 0.14012 | 0.17077 |
| 13 | 5.1873 | 5.431 | 5.428 | 5.9937 | 5.2683 | 4.96029 | 5.46445 | 5.34579 |
| 14 | 0.1912 | 0.100 | 0.100 | 0.1000 | 0.9685 | 1.0738 | 0.10000 | 0.13973 |
| 15 | 6.2410 | 6.428 | 6.427 | 8.1561 | 6.0473 | 5.9785 | 6.46445 | 6.35142 |
| 16 | 0.6994 | 0.571 | 0.581 | 0.2712 | 0.7825 | 0.78629 | 0.56255 | 0.57246 |
| 17 | 0.1158 | 0.156 | 0.151 | 11.1520 | 0.5920 | 0.73743 | 0.16711 | 0.99368 |
| 18 | 7.7643 | 7.961 | 7.973 | 7.1263 | 8.1858 | 7.3809 | 7.98901 | 7.96649 |
| 19 | 0.1000 | 0.100 | 0.100 | 4.4650 | 1.0362 | 0.66740 | 0.10000 | 0.15717 |
| 20 | 8.8279 | 8.959 | 8.974 | 9.1643 | 9.2062 | 8.3000 | 8.98901 | 8.96486 |
| 21 | 0.6986 | 0.722 | 0.719 | 2.7617 | 1.4774 | 1.19672 | 0.73575 | 1.08764 |
| 22 | 1.5563 | 0.491 | 0.422 | 0.5541 | 1.8336 | 1.0000 | 0.68113 | 0.16262 |
| 23 | 10.9806 | 10.909 | 10.892 | 16.1640 | 10.6110 | 10.8262 | 11.0695 | 11.3211 |
| 24 | 0.1317 | 0.101 | 0.100 | 0.4974 | 0.9851 | 0.1000 | 0.10000 | 0.54829 |
| 25 | 12.1492 | 11.985 | 11.887 | 16.2250 | 12.5090 | 11.6976 | 12.0695 | 12.3220 |
| 26 | 1.6373 | 1.084 | 1.040 | 1.0042 | 1.9755 | 1.3880 | 1.22229 | 1.24108 |
| 27 | 5.0032 | 6.464 | 6.646 | 3.6098 | 4.5149 | 4.9523 | 5.90240 | 5.95961 |
| 28 | 9.3545 | 10.802 | 10.801 | 8.3684 | 9.8000 | 8.8000 | 10.3914 | 10.0298 |
| 29 | 15.0919 | 13.936 | 13.870 | 15.5620 | 14.5310 | 14.6645 | 14.2710 | 14.5914 |
| Weight (lb) | 25447.1 | 25542.5 | 25491.9 | 44081.4 | 28537.8 | 25156.5 | 25519.03 | 26454.10 |
| Number of structural analyses | 48000 | 22851 | 19670 | 150000 | 150000 | 9875 | 9700 | 8900 |

as follows:

$$\begin{cases} \sigma_{\text{up}} = 0.6F_y & \text{for } \sigma_i > 0 \\ \sigma_i^b & \text{for } \sigma_i < 0 \end{cases} \tag{13}$$

$$\sigma_i^b = \begin{cases} \dfrac{\left[\left(1-\frac{\lambda_i^2}{2C_c^2}\right)F_y\right]}{\left(\frac{5}{3}+\frac{3\lambda_i}{8C_c}-\frac{\lambda_i^3}{8C_c^3}\right)} & \text{for } \lambda_i < C_c \\ \dfrac{12\pi^2 E}{23\lambda_i^2} & \text{for } \lambda_i \geq C_c \end{cases} \tag{14}$$

where $F_y$ is the yield stress of steel; $E$ is Young's modulus of elasticity of steel; $\lambda_i$ is slenderness ratio ($\lambda_i = kL_i/r_i$) ; $k$ is the effective length factor, $L_i$ is the length of each member $i$; $r_i$ is the radius of gyration of member $i$; and $C_c$ is defined as:

$$C_c = \sqrt{\frac{2\pi^2 E}{F_y}}. \tag{15}$$

**Table 12.** Comparison of optimal design for the 120-bar spatial truss structure.

| Variables | | Optimal cross-sectional areas (in.$^2$) | | | | |
|---|---|---|---|---|---|---|
| | | Lee and Geem[16] | Kaveh and Talatahari [41] | | | This study |
| | | HS | PSO | PSOPC | HPSACO | PSOST |
| **Case 1** | | | | | | |
| 1 | $A_1$ | 3.295 | 3.147 | 3.235 | 3.311 | 3.297434 |
| 2 | $A_2$ | 2.396 | 6.376 | 3.370 | 3.438 | 2.396362 |
| 3 | $A_3$ | 3.874 | 5.957 | 4.116 | 4.147 | 3.872541 |
| 4 | $A_4$ | 2.571 | 4.806 | 2.784 | 2.831 | 2.571893 |
| 5 | $A_5$ | 1.150 | 0.775 | 0.777 | 0.775 | 1.154984 |
| 6 | $A_6$ | 3.331 | 13.798 | 3.343 | 3.474 | 3.333384 |
| 7 | $A_7$ | 2.784 | 2.452 | 2.454 | 2.551 | 2.787431 |
| Weight (lb) | | 19707.07 | 32432.9 | 19618.7 | 19491.3 | 19716.89 |
| Number of structural analyses | | 35000 | 150000 | 150000 | 10025 | 6200 |
| **Case 2** | | | | | | |
| 1 | $A_1$ | 3.296 | 15.987 | 3.083 | 3.779 | 3.298311 |
| 2 | $A_2$ | 2.789 | 9.599 | 3.639 | 3.377 | 2.78323 |
| 3 | $A_3$ | 3.872 | 7.467 | 4.095 | 4.125 | 3.873659 |
| 4 | $A_4$ | 2.570 | 2.790 | 2.765 | 2.734 | 2.572721 |
| 5 | $A_5$ | 1.149 | 4.324 | 1.776 | 1.609 | 1.153868 |
| 6 | $A_6$ | 3.331 | 3.294 | 3.779 | 3.533 | 3.333883 |
| 7 | $A_7$ | 2.781 | 2.479 | 2.438 | 2.539 | 2.786458 |
| Weight (lb) | | 19893.34 | 41052.7 | 20681.7 | 20078.0 | 19906.99 |
| Number of structural analyses | | 35000 | 150000 | 150000 | 10075 | 5900 |

For this structure, the Young's modulus of elasticity was 30,450 ksi; the material density was 0.288 lb/in$^3$; and $F_y$ was considered as 58.0 ksi. The radius of gyration was expressed in terms of cross-sectional areas as $r_i = aA_i^b$ [46]. Here, $a$ and $b$ are the constants depending on the types of sections adopted for the members such as pipes, angles, and tees. For pipe sections considered in this study, $a = 0.4993$ and $b = 0.6777$ were adopted. Design variables, i.e. cross sectional areas, were categorized in seven groups shown in Figure 16. The minimum cross-sectional area was 0.775 in$^2$. The loading condition on the spatial truss was taken as vertically downward loads as follows:

-13.49 kips at node 1,

-6.744 kips at node 2 through 14;

-2.248 kips at the rest of the nodes.

The truss was analyzed for two cases: Case 1 in which no nodal displacement constraints were considered; and Case 2 in which a value of ±0.1969 inches was considered for displacement limitations of all nodes in any direction.

Table 12 gives a comparison of the best solution vectors obtained by PSOST and those obtained by Lee and Greem [16] and Kaveh and Talatahari [41].

Structural analyses show that PSOST gives the only absolutely feasible solution for this problem. Optimal weights of 19716.89 lb and 19906.99 lb are found by PSOST for Case 1 and Case 2, respectively. Figures 17 and 18 compare the rate of convergence of PSOST with PSO, PSOPC and HPSACO for Cases 1 and 2, respectively. The PSOST technique finds the absolutely feasible solution after 6200 and 5900 analyses for Cases 1 and 2, respectively, which shows a remarkable improvement in convergence rate in addition to improving the quality of the solution.

## 6. Conclusion

An innovative technique for weight optimization of pin-connected structures is proposed in this paper. The method is based on defining the concept of similar

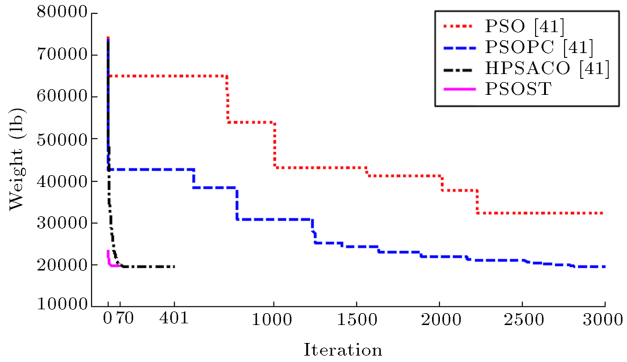


**Figure 17.** Comparison of the convergence rates between four algorithms for the 120-bar spatial truss structure (Case 1).

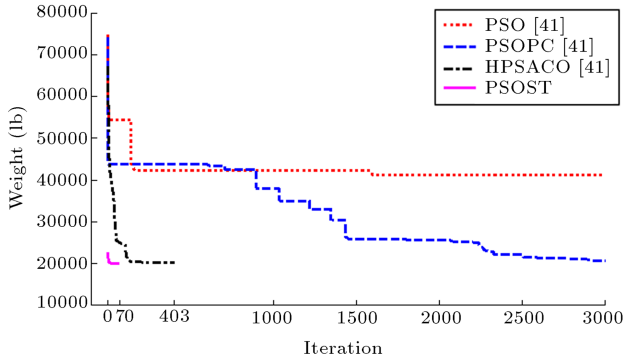


**Figure 18.** Comparison of the convergence rates between four algorithms for the 120-bar spatial truss structure (Case 2).

trusses and optimum similar trusses in optimization of truss structures. Searching Optimum Similar Trusses (SOST) is much faster and easier than searching global optimum, which is hard to find in complex real life problems. Since the number of optimum similar trusses in the search space is infinite, the procedure of finding one of the optimum similar trusses converges very rapidly. Once an optimum similar truss is found, the optimum truss can be determined by scaling it to feasible boundary of problem-specified constraints boundary (solution boundary). The effectiveness and robustness of the method were investigated through weight optimization of several pin-connected structures. The results show considerable improvement both in accuracy and particularly in the rate of convergence, compared to other techniques. As has been reported by Li et al. [37] and Degertekin [20] for most problems studied in this paper, the numbers of structural analyses required for convergence were approximately 150,000 for PSO and 125,000 for PSOPC and HPSO. In the proposed PSOST, for most problems, only 7000 analyses are required which shows a value more than 90% reduction in the number of analyses. Regardless of the difficulty of the problem, fast and rapid convergence was achieved in all tests. The proposed procedure finds an absolutely feasible solution in which no tolerance in design constraints is allowed. The advantages of this new technique can be summarized as follows:

1. Remarkable improvement in the rate of convergence and number of analyses;
2. Finding absolutely feasible solutions with no tolerance in satisfying problem-specified constraints;
3. Improving the value of objective function by finding optimum solutions which are exactly located on the solution boundary;
4. Capturing good solutions even in the early iterations;
5. Minor difference in the best and worst solutions;
6. Simplicity and robustness.

Because of the generality of the technique, the method sounds to be applicable in conjunction with other optimization algorithms such as GA, ACO and HS.

## References

1. Adeli, H. and Kumar, S. "Distributed genetic algorithm for structural optimization", *J. Aerospace Eng.*, **8**, pp. 156-163 (1995).
2. Hajela, P. and Lee, E. "Genetic algorithms in truss topological optimization", *Int. J. Solids Struct.*, **32**, pp. 3341-3357 (1995).
3. Oshaki, M. "Genetic algorithms for topology design optimization trusses", *Comput. Struct.*, **57**, pp. 219-225 (1995).
4. Wu, S.J. and Chow, P.T. "Integrated discrete and configuration optimization of trusses using genetic algorithms", *Comput. Struct.*, **55**, pp. 695-702 (1995).
5. Rajeev, S. and Krishnamoorthy, C.S. "Genetic algorithms-based methodologies for design optimization of trusses", *J. Struct. Eng.*, **123**, pp. 350-358 (1997).
6. Sarma, K.C.and Adeli, H. "Fuzzy genetic algorithm for optimization of steel structures", *J. Struct. Eng.*, **126**, pp. 596-604 (2000).
7. Deb, K. and Gulati, S. "Design of truss-structures for minimum weight using genetic algorithms", *Finite Elem. Anal.*, **37**, pp. 447-465 (2001).
8. Kaveh, A. and Kalatjari, V. "Genetic algorithm for discrete sizing optimal design of trusses using the force method", *Int. J. Numer. Methods Eng.*, **55**, pp. 55-72 (2002).
9. Kaveh, A. and Kalatjari, V. "Topology optimization of trusses using genetic algorithm, force method, and graph theory", *Int. J. Numer Methods Eng.*, **58**, pp. 771-791 (2003).

10. Kaveh, A. and Rahami, H. "Analysis, design and optimization of structures using force method and genetic algorithm", *Int. J. Numer Methods Eng.*, **65**, pp. 1570-1584 (2006).

11. Togan, V. and Daloglu, A.T. "Optimization of 3d trusses with adaptive approach in genetic algorithms", *Eng. Struct.*, **28**, pp. 1019-1027 (2006).

12. Camp, C.V. and Bichon, J. "Design of space trusses using ant colony optimization", *J. Struct. Eng.*, **130**, pp. 741-751 (2004).

13. Serra, M. and Venini, P. "On some applications of ant colony optimization metaheuristic to plane truss optimization", *Struct. Multidisc. Optim.*, **32**, pp. 499-506 (2006).

14. Kaveh, A., Farahmand Azar, B. and Talatahari, S. "Ant colony optimization for design of space trusses", *Int. J. Space Struct.*, **23**, pp. 167-181 (2008).

15. Luh, G.C. and Lin, C.Y. "Optimal design of truss structures using ant algorithm", *Struct. Multidisc Optim.*, **36**, pp. 365-379 (2008).

16. Lee, K.S. and Geem, Z.W. "A new structural optimization method based on the harmony search algorithm", *Comput. Struct.*, **82**, pp. 781-798 (2004).

17. Saka, M.P. "Optimum geometry design of geodesic domes using harmony search algorithm", *Adv. Struct. Eng.*, **10**, pp. 595-606 (2007).

18. Lamberti, L. and Pappalettere, C. "An improved harmony-search algorithm for truss structure optimization", In *Proceedings of the Twelfth International Conference Civil, Structural and Environmental Engineering Computing*, B.H.V. Topping, L.F.C. Neves and R.C. Barros, Eds., Stirlingshire, Scotland, Civil-Comp Press (2009).

19. Kaveh, A. and Talatahari, S. "A particle swarm ant colony optimization for truss structures with discrete variable", *J. Construct. Steel Res.*, **65**, pp. 1558-1568 (2009).

20. Degertekin, S.O. "Improved harmony search algorithms for sizing optimization of truss structures", *Comput. Struct.*, **92**, pp. 229-241 (2012).

21. Hasanceby, O. and Erbatur, F. "Layout optimization of trusses using simulated annealing", *Adv Eng. Software*, **33**, pp. 681-696 (2002).

22. Lamberti, L. "An efficient simulated annealing algorithm for design optimization of truss structures", *Comput. Struct.*, **86**, pp. 1936-1953 (2008).

23. Adeli, H. and Kamal, O. "Efficient optimization of space trusses", *Comput. Struct.*, **24**, pp. 501-511 (1986).

24. Adeli, H. and Kamal, O. "Efficient optimization of plane trusses", *Adv. Eng. Software*, **13**, pp. 116-122 (1991).

25. Camp, C.V. "Design of space trusses using big bang-big crunch optimization", *J. Struct. Eng.*, **87**, pp. 267-283 (2007).

26. Kaveh, A. and Talatahari, S. "Size optimization of space trusses using big-bang bigcrunch algorithm", *Comput. Struct.*, **17**, pp. 1129-40 (2009).

27. Luh, G.C. and Chueh, C.H. "Multi-objective optimal design of truss structures with immune algorithm", *Comput. Struct.*, pp. 829-844 (2004).

28. Sonmez, M. "Artificial bee colony algorithm for optimization of truss structures", *Appl. Soft Comput.*, **11**, pp. 2406-2418 (2011).

29. Kennedy, J. and Eberhart, R.C. "Particle swarm optimization", In *IEEE International Conference on Neural Networks*, Piscataway, NJ, pp. 1942-1948 (1995).

30. Hassan, R., Cohanim, B., Weck, O. and Venter, G. "A comparison of particle swarm optimization and the genetic algorithm", In *1st AIAA Multidisciplinary Design Optimization Specialist Conference*, Austin, TX (2005).

31. Hu, X., Eberhart, R. and Shi, Y. "Engineering optimization with particle swarm", In *IEEE Swarm Intelligence Symposium*, Indianapolis, pp. 53-57 (2003).

32. Yang, X.S., *Introduction to Mathematical Optimization from Linear Programming to Metaheuristics*, Cambridge International Science Publication (2008).

33. Fourie, P.C. and Groenwold, A.A. "The particle swarm optimization algorithm in size and shape optimization", *Struct. Multidisc. Optim.*, **23**, pp. 259-267 (2002).

34. Schutte, J.J. and Groenwold, A.A. "Sizing design of truss structures using particle swarms", *Struct. Multidisc. Optim.*, **25**, pp. 261-269 (2003).

35. He, S., Prempain, E. and Wu, Q.H. "An improved particle swarm optimizer for mechanical design optimization problems", *Eng. Optimiz.*, **36**, pp. 585-605 (2004).

36. Perez, R.E. and Behdinan, K. "Particle swarm approach for structural design optimization", *Comput. Struct.*, **85**, pp. 1579-1588 (2007).

37. Li, L.J., Huang, Z.B., Liu, F. and Wu, Q.H. "A heuristic particle swarm optimizer for optimization of pin connected structures", *Comput. Struct.*, **85**, pp. 340-349 (2007).

38. Li, L.J., Huang, Z.B. and Liu, F. "A heuristic particle swarm optimization method for truss structures with discrete variables", *Comput. Struct.*, **87**, pp. 435-443 (2009).

39. Luh, G.C. and Lin, C.Y. "Optimal design of truss structures using particle swarm optimization", *Comput. Struct.*, **89**, pp. 2221-2232 (2011).

40. He, S., Wu, Q.H., Wen, J.Y., Saunders, J.R. and Paton, R.C. "A particle swarm optimizer with passive congregation", *Biosystem*, **78**, pp. 135-147 (2004).

41. Kaveh, A. and Talatahari, S. "Particle swarm optimizer, ant colony strategy and harmony search scheme hybridized for optimization of truss structures", *Comput. Struct.*, **87**, pp. 267-283 (2009).

42. Sedaghati, R. "Benchmark case studies in structural design optimization using the force method", *Int. J. Solids Struct.*, **42**, pp. 5848-587164 (2005).

43. Farshi, B. and Alinia-ziazi, A. "Sizing optimization of truss structures by method of centers and force formulation", *Int. J. Solids Struct.*, **47**, pp. 2508-2524 (2010).

44. Schmit, L.A. and Farshi, B. "Some approximation concepts for structural synthesis", *AIAA J.*, **12**, pp. 692-699 (1974).

45. American Institute of Steel Construction (AISC), "Manual of steel construction allowable stress design", 9th Ed., Chicago (1989).

46. Saka, M.P. "Optimum design of pin-jointed steel structures with practical applications", *J. Struct. Eng.*, **116**, pp. 2599-2620 (1990).

## Biographies

**Abdolhossein Baghlani** is currently the Assistant Professor of Shiraz University of Technology, Shiraz, Iran. He received his BS degree in Civil Engineering, his MS and PhD degrees in Civil Engineering, Hydraulic Structures, at Shiraz University, Shiraz, Iran, in 1995, 1998 and 2007 respectively. His areas of research and interest are optimization in civil engineering problems, computational fluid dynamics, numerical methods, hydraulic structures, and sediment transport.

**Mohammad Hadi Makiabadi** is currently the MSc graduate student of earthquake engineering from Shiraz University of Technology, Shiraz, Iran. His areas of research and interest are earthquake engineering, structural optimization, seismic behavior of structures, and reliability analysis.